

*Electronic Supplementary Information*

**A novel self-assembled supramolecular sensor based on  
thiophene functionalized imidazophenazine for dual-channel  
detection Ag<sup>+</sup> in aqueous solution**

Hai-Xiong Shi, Wen-Ting Li, Qiao Li, Hai-Li Zhang, Tai-Bao Wei\*, You-Ming

Zhang, Qi Lin and Hong Yao

*Key Laboratory of Eco-Environment-Related Polymer Materials, Ministry of*

*Education of China; Key Laboratory of Polymer Materials of Gansu Province;*

*College of Chemistry and Chemical Engineering, Northwest Normal University,*

*Lanzhou, Gansu, 730070. P. R. China*

## Table of Contents

### Instruments and materials.

### Synthesis of sensors IM.

### General procedure for UV-vis and fluorescence spectra experiments.

### General procedure for $^1\text{H}$ NMR experiments.

**Fig. S1** UV-vis absorption and spectra of **S1** (20  $\mu\text{M}$ ) with metal ions ( $\text{Fe}^{3+}$ ,  $\text{Hg}^{2+}$ ,  $\text{Ag}^+$ ,  $\text{Ca}^{2+}$ ,  $\text{Cu}^{2+}$ ,  $\text{Co}^{2+}$ ,  $\text{Ni}^{2+}$ ,  $\text{Cd}^{2+}$ ,  $\text{Pb}^{2+}$ ,  $\text{Zn}^{2+}$ ,  $\text{Cr}^{3+}$ , and  $\text{Mg}^{2+}$ ) in the DMSO/ $\text{H}_2\text{O}$  (v:v = 1:1, buffered with HEPES pH = 7.2) solution in response to  $\text{Ag}^+$  (10 equiv.).

**Fig. S2** Fluorescence spectra responses in DMSO/ $\text{H}_2\text{O}$  (v : v = 1 : 1, buffered with HEPES pH = 7.2) of **S1** ( $2.0 \times 10^{-5}$  M) upon addition of  $\text{Pd}^{2+}$  (10 equiv.).

**Fig. S3** UV-vis absorption and spectra of **S1** (20  $\mu\text{M}$ ) with  $\text{Pd}^{2+}$  ions in the DMSO/ $\text{H}_2\text{O}$  (v:v = 1:1, buffered with HEPES pH = 7.2) solution in response to  $\text{Ag}^+$  (10 equiv.).

**Fig. S4** UV-vis absorbance intensity of **S1** (20  $\mu\text{M}$ ) in response to  $\text{Ag}^+$  (10 equiv.) in the presence of various metal ions species in DMSO/ $\text{H}_2\text{O}$  (v:v = 1:1, buffered with HEPES pH = 7.2) solution. From 1 to 13: **S1**, **S1** +  $\text{Ag}^+$ , **S1** +  $\text{Ag}^+$  +  $\text{Fe}^{3+}$ , **S1** +  $\text{Ag}^+$  +  $\text{Ca}^{2+}$ , **S1** +  $\text{Ag}^+$  +  $\text{Cu}^{2+}$ , **S1** +  $\text{Ag}^+$  +  $\text{Co}^{2+}$ , **S1** +  $\text{Ag}^+$  +  $\text{Ni}^{2+}$ , **S1** +  $\text{Ag}^+$  +  $\text{Cd}^{2+}$ , **S1** +  $\text{Ag}^+$  +  $\text{Pb}^{2+}$ , **S1** +  $\text{Ag}^+$  +  $\text{Zn}^{2+}$ , **S1** +  $\text{Ag}^+$  +  $\text{Hg}^{2+}$ , **S1** +  $\text{Ag}^+$  +  $\text{Cr}^{3+}$ , **S1** +  $\text{Ag}^+$  +  $\text{Mg}^{2+}$ .

**Fig. S5** Plot of the intensity at 365 nm for a mixture of the sensor **S1** (20  $\mu\text{M}$ ) and  $\text{Ag}^+$  in DMSO/ $\text{H}_2\text{O}$  (v:v = 1:1, buffered with HEPES pH = 7.2) in the range 0.00 to 42.24  $\mu\text{M}$ . ( $\lambda_{\text{ex}}$  = 400 nm).

**Fig. S6** Plot of the absorbance for a mixture of the sensor **S1** (20  $\mu\text{M}$ ) and  $\text{Ag}^+$  in DMSO/ $\text{H}_2\text{O}$  (v:v = 1:1, buffered with HEPES pH = 7.2) in the range 0.00 to 40.32  $\mu\text{M}$ .

**Fig. S7** The pH response of **S1** and **S1-Ag<sup>+</sup>** in the DMSO/ $\text{H}_2\text{O}$  (v:v = 1:1, buffered with HEPES pH = 7.2) solution.

**Fig. S8** XRD diagrams of **S1** and **S1-Ag<sup>+</sup>**.

**Fig. S9** Fluorescence intensity reversible switching cycles of the **S1** water solution ( $2.0 \times 10^{-5}$  M) on alternate addition of  $\text{Ag}^+$  and  $\text{I}^-$ .

**Fig. S10** FT-IR spectra of compound **S1** and **S1-Ag<sup>+</sup>**.

**Fig. S11** <sup>1</sup>H NMR spectra (600 MHz, DMSO-*d*<sub>6</sub>) of free **S1** and in the presence of Ag<sup>+</sup>.

**Fig. S12** Optimized structures of **IM**.

**Fig. S13** Optimized structures of **IM-Ag<sup>+</sup>** complexes.

**Table S1** Fluorescent sensors reported for the detection of Ag<sup>+</sup>.

**Table S2** DFT computed selected bond lengths for **IM**.

**Table S3** DFT computed selected bond angles for **IM**.

**Table S4** DFT computed selected bond lengths for **IM-Ag<sup>+</sup>**.

**Table S5** DFT computed selected bond angles for **IM-Ag<sup>+</sup>**.

**Fig. S14** ESI-MS spectrum of **IM**.

**Fig. S15** ESI-MS spectrum of **IM-Ag<sup>+</sup>**.

**Fig. S16** The Job's plot examined between Ag<sup>+</sup> and **IM**, indicating the 2 : 1 stoichiometry, which was carried out by fluorescence spectra ( $\lambda_{\text{ex}} = 400 \text{ nm}$ ).

**Fig. S17** <sup>1</sup>H NMR spectra of compound **S1**.

**Fig. S18** <sup>13</sup>C NMR spectra of compound **IM**.

## References

## Instruments and materials

$^1\text{H}$  NMR and  $^{13}\text{C}$  NMR spectra were carried out on a Mercury-400BB spectrometer at 600 MHz. Electrospray ionization mass spectra (ESI-MS) were measured on an Agilent 1100 LC-MSD-Trap-VL system. UV-visible spectra were recorded on a Shimadzu UV-2550 spectrometer. Photoluminescence spectra were performed on a Shimadzu RF-5301 fluorescence spectrophotometer. Melting points were measured on an X-4 digital melting-point apparatus (uncorrected). The infrared spectra were performed on a Digilab FTS-3000 FT-IR spectrophotometer. All cations, in terms of  $\text{Fe}^{3+}$ ,  $\text{Hg}^{2+}$ ,  $\text{Ag}^+$ ,  $\text{Ca}^{2+}$ ,  $\text{Cu}^{2+}$ ,  $\text{Co}^{2+}$ ,  $\text{Ni}^{2+}$ ,  $\text{Cd}^{2+}$ ,  $\text{Pb}^{2+}$ ,  $\text{Zn}^{2+}$ ,  $\text{Cr}^{3+}$ , and  $\text{Mg}^{2+}$  were added in the form of perchlorate salts, which were purchased from Alfa-Aesar Chemical, and stored in a vacuum desiccator containing self-indicating silica and dried fully before using. All reagents were gained commercially for synthesis and without further purification during experiment progress. Double distilled water was used throughout the experiment.

## Synthesis of sensors IM

2,3-Diamino-phenazine (0.42g, 2 mmol), 2-thiophene carboxaldehyde (0.22 g, 2 mmol) and catalytic amount of acetic acid (AcOH) were combined in hot absolute DMF (20 mL). The solution was stirred under reflux conditions for 8 h, after cooling to room temperature, the brown precipitate was filtrated, washed with hot absolute ethanol for three times, then recrystallized with DMF- $\text{H}_2\text{O}$  to get yellow powdery product **S1** (0.52g) at yield of 82% (m.p.  $>300^\circ\text{C}$ ),  $^1\text{H}$  NMR ( $\text{DMSO}-d_6$ , 600 MHz)  $\delta$ :13.50 (s 1H), 8.44 (s 1H), 8.23 (s 2H), 8.15 (m 2H), 8.00-7.99 (d 1H), 7.90-7.88 (m

2H), 7.39-7.36 (m 1H), 6.25 (s 1H).  $^{13}\text{C}$  NMR (151 MHz, DMSO- $d_6$ ),  $\delta$  155.63, 149.42, 142.34, 140.95, 132.92, 130.85 and 129.50. IR (KBr,  $\text{cm}^{-1}$ )  $\nu$ : 3428.85, 3200.52, 1655.37, 1589.50, 1565.35, 1505.34, 1427.05; ESI-MS  $m/z$ :  $[\text{M} - \text{H}^+]$  Calcd for  $\text{C}_{17}\text{H}_{10}\text{N}_4\text{S}$  301.06; Found 301.09.

### **General procedure for UV-vis and fluorescence spectra experiments**

The solution of sensor **S1** ( $2.0 \times 10^{-4}$  M) in DMSO was prepared and stored in dry atmosphere. The solution was used for all spectroscopic studies after appropriate dilution. The DMSO solutions of each cations ( $4 \times 10^{-3}$  M) were prepared, via perchloratesalts of  $\text{Fe}^{3+}$ ,  $\text{Hg}^{2+}$ ,  $\text{Ag}^+$ ,  $\text{Ca}^{2+}$ ,  $\text{Cu}^{2+}$ ,  $\text{Co}^{2+}$ ,  $\text{Ni}^{2+}$ ,  $\text{Cd}^{2+}$ ,  $\text{Pb}^{2+}$ ,  $\text{Zn}^{2+}$ ,  $\text{Cr}^{3+}$ , and  $\text{Mg}^{2+}$ . All the UV-vis experiments were carried out in DMSO/ $\text{H}_2\text{O}$  ( $v:v = 1:1$ , buffered with HEPES  $\text{pH} = 7.2$ ) solution on a Shimadzu UV-2550 spectrometer. Any change in the UV-vis spectra of the synthesized compounds was recorded on addition of salts while keeping the ligand concentration constant ( $2.0 \times 10^{-5}$  M) in all experiments. All the fluorescence spectra experiments were carried out in DMSO/ $\text{H}_2\text{O}$  ( $v:v = 1:1$ , buffered with HEPES  $\text{pH} = 7.2$ ) solution on a Shimadzu RF-5301 spectrometer. The fluorescence spectra were obtained by excitation at 400 nm. Any change in the fluorescence spectra of the synthesized compounds was recorded upon the addition of salts while keeping the ligand concentration constant ( $2.0 \times 10^{-5}$  M) in all experiments.

### **General procedure for $^1\text{H}$ NMR experiments**

For  $^1\text{H}$  NMR titrations, two stock solutions were prepared in DMSO- $d_6$ , one containing the sensor only and the second containing an appropriate concentration of

the metal. Aliquots of the two solutions were mixed directly in NMR tube.

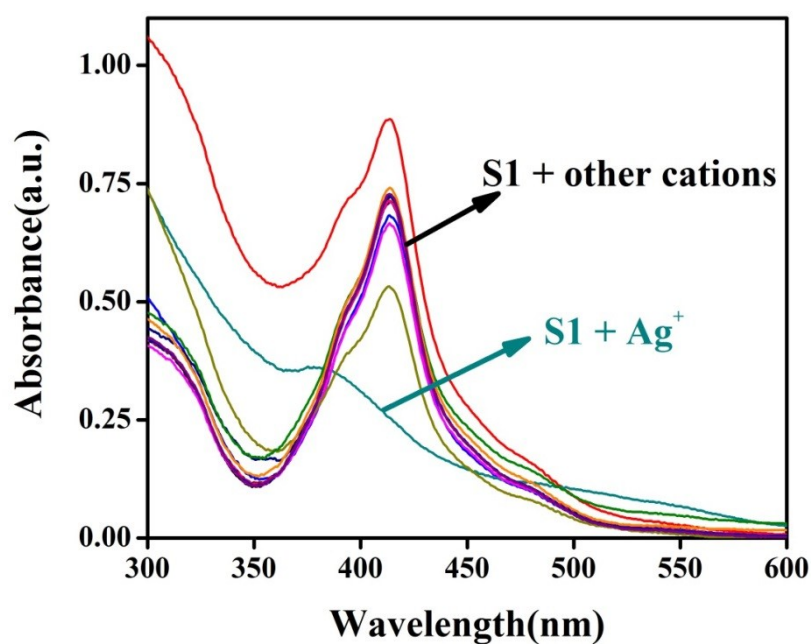


**Fig. S1** UV-vis absorption and spectra of S1 (20  $\mu$ M) with metal ions ( $\text{Fe}^{3+}$ ,  $\text{Hg}^{2+}$ ,  $\text{Ag}^+$ ,  $\text{Ca}^{2+}$ ,  $\text{Cu}^{2+}$ ,  $\text{Co}^{2+}$ ,  $\text{Ni}^{2+}$ ,  $\text{Cd}^{2+}$ ,  $\text{Pb}^{2+}$ ,  $\text{Zn}^{2+}$ ,  $\text{Cr}^{3+}$ , and  $\text{Mg}^{2+}$ ) in the DMSO/ $\text{H}_2\text{O}$  (v:v = 1:1, buffered with HEPES pH = 7.2) solution in response to  $\text{Ag}^+$  (10 equiv.).

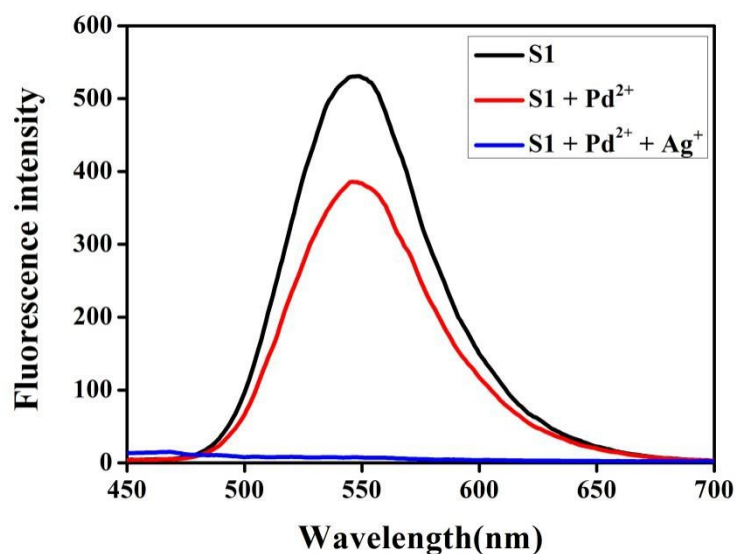


**Fig. S2** Fluorescence spectra responses in DMSO/ $\text{H}_2\text{O}$  (v : v = 1 : 1, buffered with HEPES pH = 7.2) of S1 ( $2.0 \times 10^{-5}$  M) upon addition of  $\text{Pd}^{2+}$  (10 equiv.).

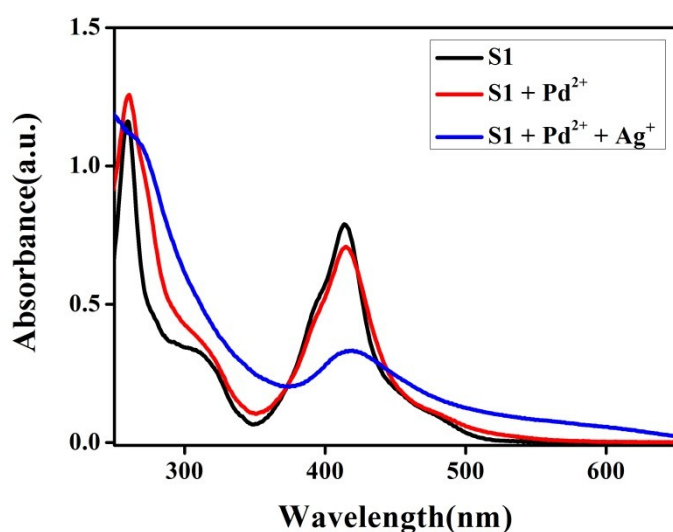


**Fig. S3** UV-vis absorption and spectra of **S1** (20  $\mu\text{M}$ ) with  $\text{Pd}^{2+}$  ions in the  $\text{DMSO}/\text{H}_2\text{O}$  (v:v = 1:1, buffered with HEPES pH = 7.2) solution in response to  $\text{Ag}^+$  (10 equiv.).

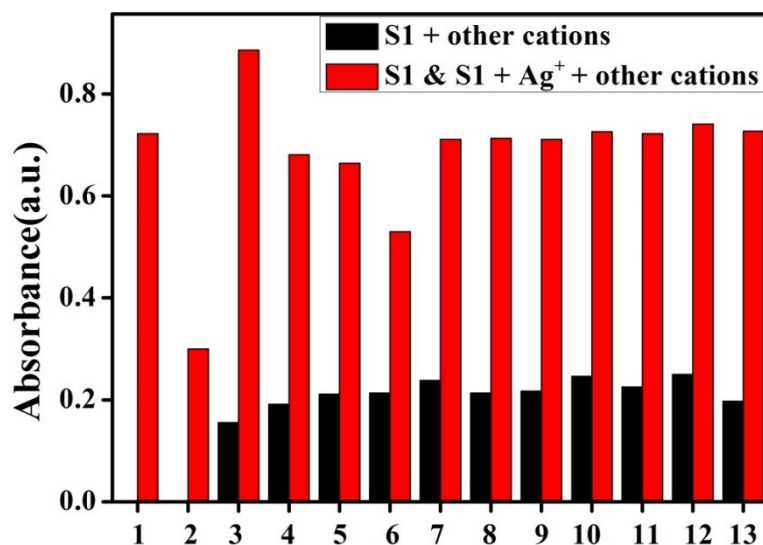


**Fig. S4** UV-vis absorbance intensity of **S1** (20  $\mu\text{M}$ ) in response to  $\text{Ag}^+$  (10 equiv.) in the presence of various metal ions species in  $\text{DMSO}/\text{H}_2\text{O}$  (v:v = 1:1, buffered with HEPES pH = 7.2) solution. From 1 to 13: **S1**, **S1** +  $\text{Ag}^+$ , **S1** +  $\text{Ag}^+$  +  $\text{Fe}^{3+}$ , **S1** +  $\text{Ag}^+$  +  $\text{Ca}^{2+}$ , **S1** +  $\text{Ag}^+$  +  $\text{Cu}^{2+}$ , **S1** +  $\text{Ag}^+$  +  $\text{Co}^{2+}$ , **S1** +  $\text{Ag}^+$  +  $\text{Ni}^{2+}$ , **S1** +  $\text{Ag}^+$  +  $\text{Cd}^{2+}$ , **S1** +  $\text{Ag}^+$  +  $\text{Pb}^{2+}$ , **S1** +  $\text{Ag}^+$  +  $\text{Zn}^{2+}$ , **S1** +  $\text{Ag}^+$  +  $\text{Hg}^{2+}$ , **S1** +  $\text{Ag}^+$  +  $\text{Cr}^{3+}$ , **S1** +  $\text{Ag}^+$  +  $\text{Mg}^{2+}$ .

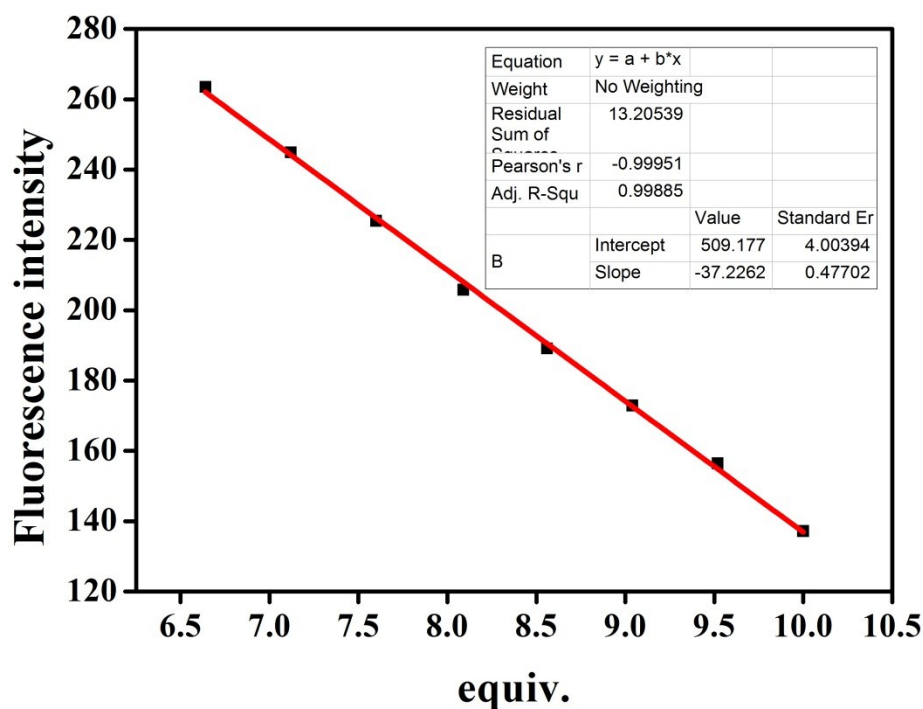


**Fig. S5** Plot of the intensity at 365nm for a mixture of the sensor **S1** (20  $\mu\text{M}$ ) and  $\text{Ag}^+$  in DMSO/ $\text{H}_2\text{O}$  (v:v = 1:1, buffered with HEPES pH = 7.2) in the range 0.00 to 42.24  $\mu\text{M}$ . ( $\lambda_{\text{ex}}$  = 400 nm). The result of the analysis as follows:

Linear Equation:  $Y = -37.2262 \times X + 509.177$   $R^2 = 0.99885$

$$S = 37.2262 \times 10^6 \quad \delta = \sqrt{\frac{\sum(A_0 - A_1)^2}{N-1}} = 0.1016 (N=20) \quad K = 3$$

$$\text{LOD} = K \times \delta / S = 8.18 \times 10^{-9} \text{ M}$$

$A_0$  is the absorbance intensity of **S1**;  $A_1$  is the average of the  $A_0$ .



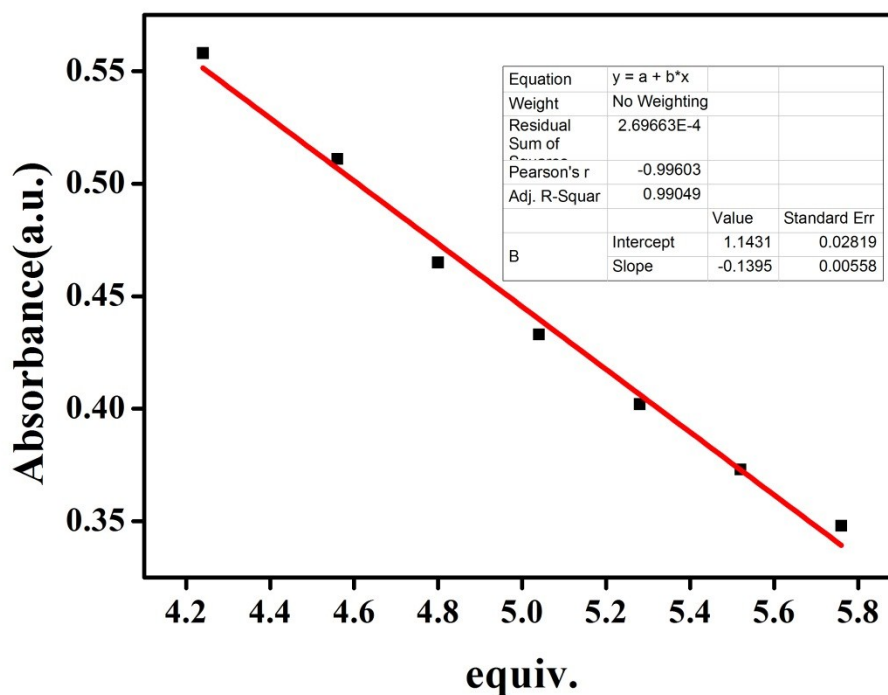


**Fig. S6** Plot of the absorbance for a mixture of the sensor **S1** (20  $\mu\text{M}$ ) and  $\text{Ag}^+$  in DMSO/ $\text{H}_2\text{O}$  (v:v = 1:1, buffered with HEPES pH = 7.2) in the range 0.00 to 40.32  $\mu\text{M}$ . The result of the analysis as follows:

Linear Equation:  $Y = -0.1395 \times X + 1.1431$   $R^2 = 0.99603$

$S = 0.1395 \times 10^6$   $\delta = \sqrt{\frac{\sum(A_0 - A_1)^2}{N-1}} = 0.040694 (N=20)$   $K = 3$

$\text{LOD} = K \times \delta / S = 8.75 \times 10^{-7} \text{ M}$

$A_0$  is the absorbance intensity of **S1**;  $A_1$  is the average of the  $A_0$ .

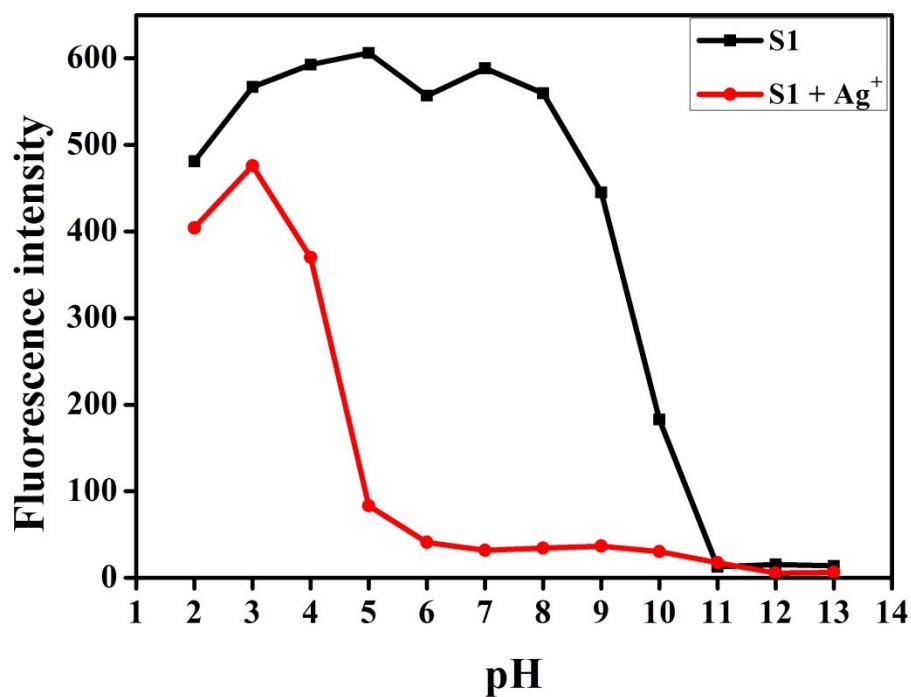


**Fig. S7** The pH response of S1 and S1-Ag<sup>+</sup> in the DMSO/H<sub>2</sub>O (v:v = 1:1, buffered with HEPES pH = 7.2) solution.

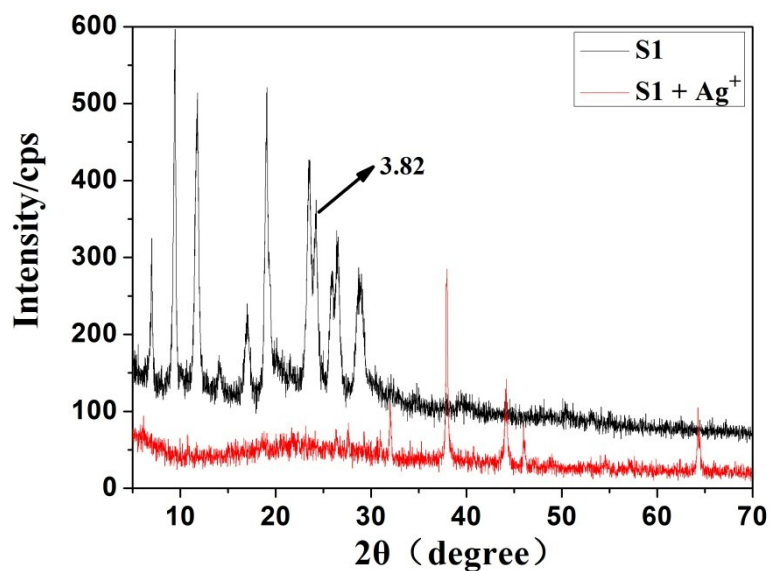


**Fig. S8** XRD diagrams of S1 and S1-Ag<sup>+</sup>.

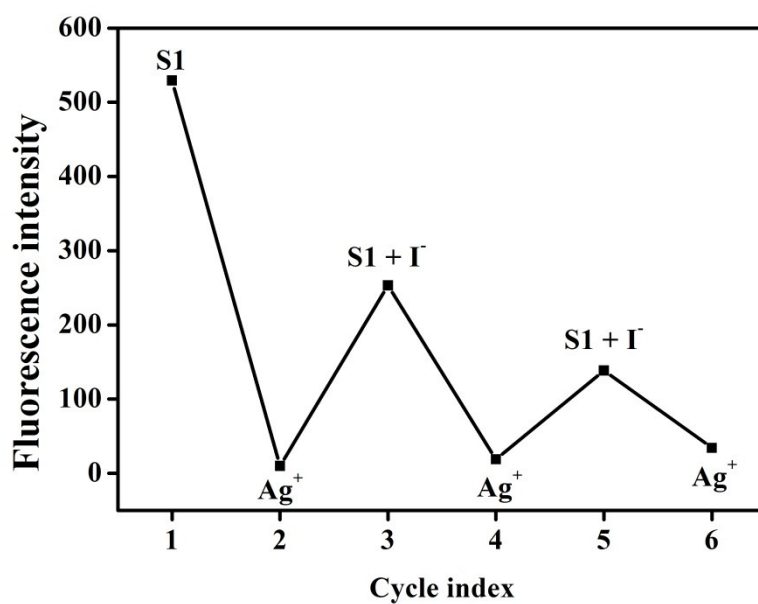


**Fig. S9** Fluorescence intensity reversible switching cycles of the S1 water solution ( $2.0 \times 10^{-5}$  M) on alternate addition of Ag<sup>+</sup> and I<sup>-</sup>.

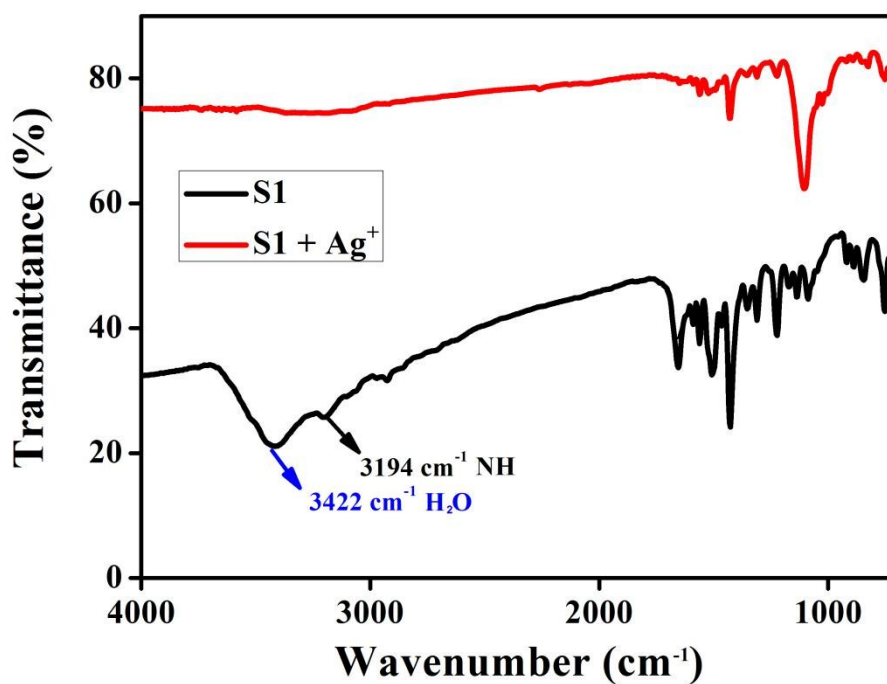


**Fig. S10** FT-IR spectra of compound S1 and S1-Ag<sup>+</sup>.

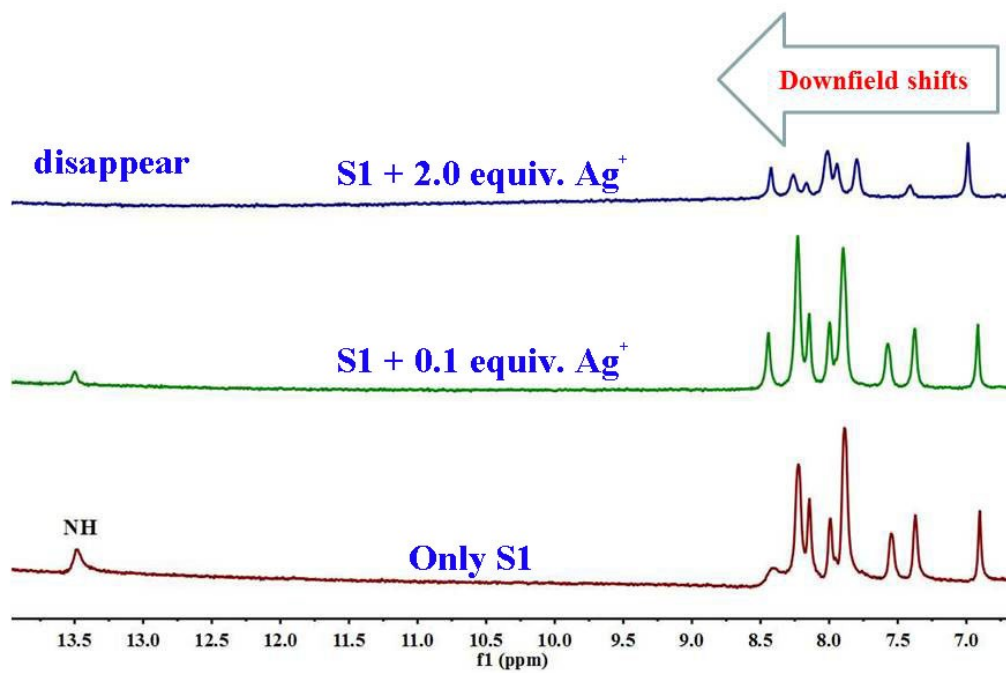


**Fig. S11** <sup>1</sup>H NMR spectra (600 MHz, DMSO-*d*<sub>6</sub>) of free S1 and in the presence of Ag<sup>+</sup>.

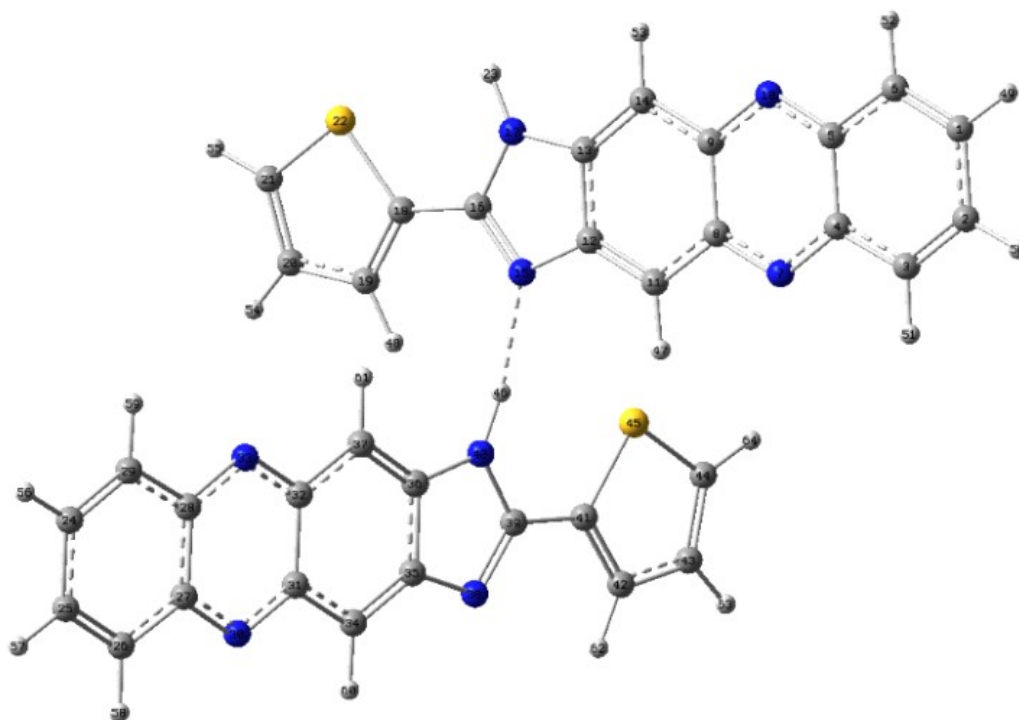


**Fig. S12** Optimized structures of IM.

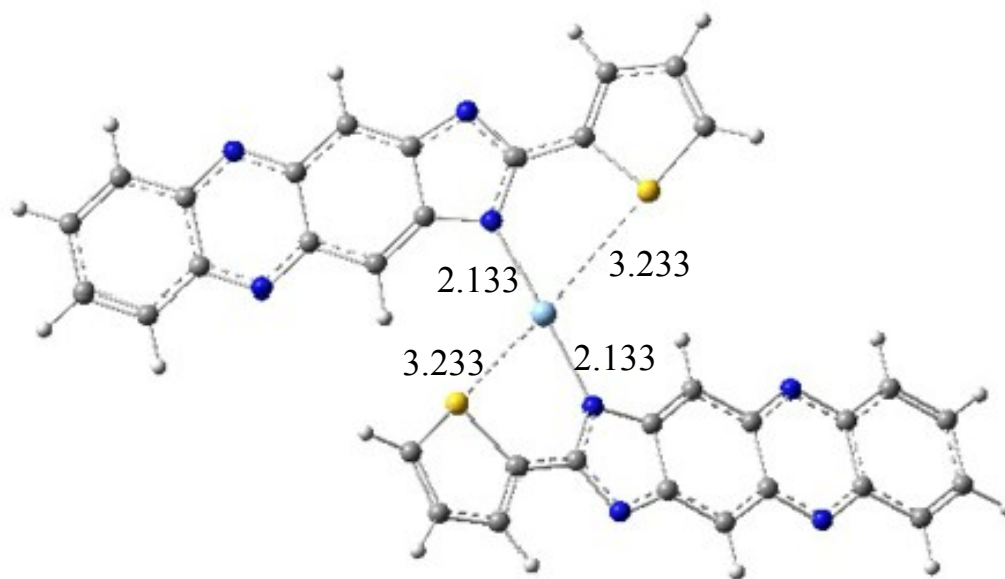


**Fig. S13** Optimized structures of **IM-Ag<sup>+</sup>** complexes.

**Table S1** Fluorescent sensors reported for the detection of **Ag<sup>+</sup>**.

References	Reproducibility	LOD (M)	Solvent	Selectivity
[1]	No	$4.0 \times 10^{-9}$	Ethanol	Ag <sup>+</sup>
[2]	No	$5.0 \times 10^{-8}$	DMSO/H <sub>2</sub> O (v/v, 9:1)	Ag <sup>+</sup>
[3]	No	$6.20 \times 10^{-6}$	CH <sub>3</sub> CN/H <sub>2</sub> O (v/v, 1:1)	Ag <sup>+</sup>
[4]	No	$6.0 \times 10^{-7}$	H <sub>2</sub> O	Ag <sup>+</sup>
[5]	More than 3 times	$7.73 \times 10^{-8}$	DMSO/H <sub>2</sub> O (v/v, 1:1)	Ag <sup>+</sup>
This work	3 times	$8.18 \times 10^{-9}$	DMSO/H <sub>2</sub> O (v/v, 1:1)	Ag <sup>+</sup>

**Table S2** DFT computed selected bond lengths for **IM**.

<b>Chemical bond</b>	<b>Bond length/(10<sup>-10</sup> m)</b>	<b>Chemical bond</b>	<b>Bond length/(10<sup>-10</sup> m)</b>	<b>Chemical bond</b>	<b>Bond length/(10<sup>-10</sup> m)</b>	<b>Chemical bond</b>	<b>Bond length/(10<sup>-10</sup> m)</b>
R(1,2)	1.418	R(1,6)	1.3779	R(1,46)	1.0851	R(2,3)	1.3843
R(2,47)	1.0856	R(3,4)	1.4138	R(3,48)	1.0848	R(4,5)	1.4441
R(4,7)	1.3562	R(5,6)	1.4253	R(5,10)	1.3431	R(6,49)	1.0849
R(7,8)	1.3286	R(8,9)	1.4607	R(8,11)	1.4407	R(9,10)	1.3428
R(9,14)	1.4177	R(11,12)	1.3706	R(11,50)	1.0854	R(12,13)	1.4499
R(12,15)	1.3826	R(13,14)	1.3976	R(13,17)	1.3471	R(14,51)	1.0845
R(15,16)	1.3617	R(15,45)	2.1266	R(16,17)	1.3639	R(16,18)	1.4403
R(18,19)	1.3854	R(18,22)	1.7527	R(19,20)	1.4143	R(19,52)	1.0842
R(20,21)	1.3775	R(20,53)	1.0833	R(21,22)	1.7194	R(21,54)	1.0819
R(23,24)	1.4183	R(23,28)	1.384	R(23,55)	1.0856	R(24,25)	1.3777
R(24,56)	1.0851	R(25,26)	1.4255	R(25,57)	1.0849	R(26,27)	1.4443
R(26,29)	1.3429	R(27,28)	1.4141	R(27,32)	1.3558	R(28,58)	1.0848
R(29,30)	1.3431	R(30,31)	1.4606	R(30,33)	1.4175	R(31,32)	1.3288
R(31,36)	1.4404	R(33,34)	1.3978	R(33,59)	1.0845	R(34,35)	1.45
R(34,37)	1.348	R(35,36)	1.3703	R(35,39)	1.3827	R(36,60)	1.0855
R(37,38)	1.3635	R(38,39)	1.3616	R(38,40)	1.4405	R(39,45)	2.1278
R(40,41)	1.3845	R(40,44)	1.7497	R(41,42)	1.4162	R(41,61)	1.0826
R(42,43)	1.3728	R(42,62)	1.0833	R(43,44)	1.7311	R(43,63)	1.0815

**Table S3** DFT computed selected bond angles for **IM**.

<b>Bond angle</b>	<b>Angle/°</b>	<b>Bond angle</b>	<b>Angle/°</b>	<b>Bond angle</b>	<b>Angle/°</b>
A(2,1,6)	120.4738	A(2,1,46)	119.4293	A(6,1,46)	120.0969
A(1,2,3)	121.0959	A(1,2,47)	119.2574	A(3,2,47)	119.6468
A(2,3,4)	119.9675	A(2,3,48)	121.8157	A(4,3,48)	118.2168
A(3,4,5)	119.1093	A(3,4,7)	119.5132	A(5,4,7)	121.3775
A(4,5,6)	119.4099	A(4,5,10)	121.3586	A(6,5,10)	119.2316
A(1,6,5)	119.9436	A(1,6,49)	122.1907	A(5,6,49)	117.8657
A(4,7,8)	117.3548	A(7,8,9)	121.2693	A(7,8,11)	118.4534
A(9,8,11)	120.2773	A(8,9,10)	121.3611	A(8,9,14)	120.1786
A(10,9,14)	118.4603	A(5,10,9)	117.2787	A(8,11,12)	118.167
A(8,11,50)	118.0939	A(12,11,50)	123.7391	A(11,12,13)	121.6983
A(11,12,15)	131.6499	A(13,12,15)	106.6509	A(12,13,14)	121.4714
A(12,13,17)	109.497	A(14,13,17)	129.0317	A(9,14,13)	118.2069
A(9,14,51)	119.7279	A(13,14,51)	122.0652	A(12,15,16)	104.6061
A(12,15,45)	123.3185	A(16,15,45)	131.9418	A(15,16,17)	114.8109
A(15,16,18)	125.8876	A(17,16,18)	119.2997	A(13,17,16)	104.4332
A(16,18,19)	130.7173	A(16,18,22)	118.5193	A(19,18,22)	110.7562
A(18,19,20)	113.106	A(18,19,52)	123.5561	A(20,19,52)	123.3256
A(19,20,21)	112.3134	A(19,20,53)	124.1256	A(21,20,53)	123.5597
A(20,21,22)	112.6167	A(20,21,54)	127.5504	A(22,21,54)	119.8325
A(18,22,21)	91.2064	A(24,23,28)	121.087	A(24,23,55)	119.2573
A(28,23,55)	119.6557	A(23,24,25)	120.4884	A(23,24,56)	119.4189
A(25,24,56)	120.0927	A(24,25,26)	119.9515	A(24,25,57)	122.1853
A(26,25,57)	117.8631	A(25,26,27)	119.3859	A(25,26,29)	119.2394
A(27,26,29)	121.3747	A(26,27,28)	119.118	A(26,27,32)	121.3678
A(28,27,32)	119.5142	A(23,28,27)	119.9692	A(23,28,58)	121.8264
A(27,28,58)	118.2045	A(26,29,30)	117.2841	A(29,30,31)	121.3258
A(29,30,33)	118.475	A(31,30,33)	120.1992	A(30,31,32)	121.2971
A(30,31,36)	120.244	A(32,31,36)	118.4588	A(27,32,31)	117.3504
A(30,33,34)	118.2557	A(30,33,59)	119.677	A(34,33,59)	122.0672
A(33,34,35)	121.3536	A(33,34,37)	128.9537	A(35,34,37)	109.6926
A(34,35,36)	121.7814	A(34,35,39)	106.5054	A(36,35,39)	131.7126
A(31,36,35)	118.1654	A(31,36,60)	118.0518	A(35,36,60)	123.7822
A(34,37,38)	104.2122	A(37,38,39)	114.9622	A(37,38,40)	119.5105
A(39,38,40)	125.527	A(35,39,38)	104.6272	A(35,39,45)	123.9543
A(38,39,45)	131.4119	A(38,40,41)	125.4435	A(38,40,44)	123.8537
A(41,40,44)	110.7025	A(40,41,42)	113.1482	A(40,41,61)	121.7707
A(42,41,61)	125.0811	A(41,42,43)	112.7268	A(41,42,62)	124.038
A(43,42,62)	123.2352	A(42,43,44)	112.0393	A(42,43,63)	128.3543
A(44,43,63)	119.6058	A(40,44,43)	91.3831		

**Table S4** DFT computed selected bond lengths for **IM-Ag<sup>+</sup>**.

<b>Chemical bond</b>	<b>Bond length/(10<sup>-10</sup> m)</b>	<b>Chemical bond</b>	<b>Bond length/(10<sup>-10</sup> m)</b>	<b>Chemical bond</b>	<b>Bond length/(10<sup>-10</sup> m)</b>	<b>Chemical bond</b>	<b>Bond length/(10<sup>-10</sup> m)</b>
R(1,2)	1.4298	R(1,6)	1.3688	R(1,49)	1.0859	R(2,3)	1.3684
R(2,50)	1.0859	R(3,4)	1.4303	R(3,51)	1.085	R(4,5)	1.448
R(4,7)	1.3383	R(5,6)	1.4295	R(5,10)	1.3396	R(6,52)	1.085
R(7,8)	1.346	R(8,9)	1.4591	R(8,11)	1.4221	R(9,10)	1.3446
R(9,14)	1.424	R(11,12)	1.3758	R(11,47)	1.0836	R(12,13)	1.441
R(12,15)	1.3906	R(13,14)	1.3701	R(13,17)	1.3855	R(14,53)	1.0841
R(15,16)	1.321	R(15,46)	1.9384	R(16,17)	1.3821	R(16,18)	1.4476
R(17,23)	1.0082	R(18,19)	1.3784	R(18,22)	1.7527	R(19,20)	1.4198
R(19,48)	1.0825	R(20,21)	1.3697	R(20,54)	1.0832	R(21,22)	1.7302
R(21,55)	1.0809	R(24,25)	1.4289	R(24,29)	1.3694	R(24,56)	1.0862
R(25,26)	1.3691	R(25,57)	1.0861	R(26,27)	1.4301	R(26,58)	1.0852
R(27,28)	1.4461	R(27,30)	1.3395	R(28,29)	1.4295	R(28,33)	1.3406
R(29,59)	1.0853	R(30,31)	1.3463	R(31,32)	1.4626	R(31,34)	1.4212
R(32,33)	1.3448	R(32,37)	1.4232	R(34,35)	1.3773	R(34,60)	1.0836
R(35,36)	1.4462	R(35,38)	1.3839	R(36,37)	1.3721	R(36,40)	1.3824
R(37,61)	1.0838	R(38,39)	1.3188	R(39,40)	1.3859	R(39,41)	1.4503
R(40,46)	1.0288	R(41,42)	1.3778	R(41,45)	1.7514	R(42,43)	1.4199
R(42,62)	1.0826	R(43,44)	1.3702	R(43,63)	1.0837	R(44,45)	1.7318
R(44,64)	1.081	R(45,48)	4.0556				



**Table S5** DFT computed selected bond angles for **IM-Ag<sup>+</sup>**.

<b>Bond angle</b>	<b>Angle/°</b>	<b>Bond angle</b>	<b>Angle/°</b>	<b>Bond angle</b>	<b>Angle/°</b>
A(2,1,6)	120.87	A(2,1,49)	119.107	A(6,1,49)	120.0231
A(1,2,3)	120.8081	A(1,2,50)	119.1266	A(3,2,50)	120.0653
A(2,3,4)	120.1969	A(2,3,51)	122.2527	A(4,3,51)	117.5504
A(3,4,5)	118.9809	A(3,4,7)	119.4579	A(5,4,7)	121.5612
A(4,5,6)	118.9472	A(4,5,10)	121.528	A(6,5,10)	119.5248
A(1,6,5)	120.1969	A(1,6,52)	122.198	A(5,6,52)	117.6051
A(4,7,8)	117.4115	A(7,8,9)	120.9677	A(7,8,11)	118.5821
A(9,8,11)	120.4501	A(8,9,10)	121.2359	A(8,9,14)	120.2297
A(10,9,14)	118.5343	A(5,10,9)	117.2956	A(8,11,12)	118.2261
A(8,11,47)	119.0823	A(12,11,47)	122.6915	A(11,12,13)	120.6005
A(11,12,15)	129.824	A(13,12,15)	109.5753	A(12,13,14)	123.442
A(12,13,17)	104.1446	A(14,13,17)	132.4135	A(9,14,13)	117.0514
A(9,14,53)	118.9015	A(13,14,53)	124.0471	A(12,15,16)	105.9652
A(12,15,46)	121.9964	A(16,15,46)	131.7492	A(15,16,17)	112.3494
A(15,16,18)	125.0787	A(17,16,18)	122.5718	A(13,17,16)	107.9649
A(13,17,23)	125.9329	A(16,17,23)	126.0436	A(16,18,19)	127.2922
A(16,18,22)	122.0369	A(19,18,22)	110.6704	A(18,19,20)	113.0751
A(18,19,48)	122.6835	A(20,19,48)	124.241	A(19,20,21)	112.953
A(19,20,54)	123.7593	A(21,20,54)	123.2877	A(20,21,22)	111.8319
A(20,21,55)	128.5624	A(22,21,55)	119.6037	A(18,22,21)	91.4686
A(25,24,29)	120.7728	A(25,24,56)	119.1753	A(29,24,56)	120.0519
A(24,25,26)	120.7258	A(24,25,57)	119.1876	A(26,25,57)	120.0865
A(25,26,27)	120.3313	A(25,26,58)	122.1797	A(27,26,58)	117.489
A(26,27,28)	118.9304	A(26,27,30)	119.4809	A(28,27,30)	121.5887
A(27,28,29)	118.9098	A(27,28,33)	121.5622	A(29,28,33)	119.528
A(24,29,28)	120.3298	A(24,29,59)	122.1423	A(28,29,59)	117.5279
A(27,30,31)	117.4489	A(30,31,32)	118.7364	A(32,31,34)	120.3548
A(31,32,33)	121.1345	A(31,32,37)	120.2248	A(33,32,37)	118.6406
A(28,33,32)	117.3567	A(31,34,35)	118.4641	A(31,34,60)	119.2495
A(35,34,60)	122.2863	A(34,35,36)	120.4561	A(34,35,38)	129.7226
A(36,35,38)	109.8212	A(35,36,37)	123.2686	A(35,36,40)	104.6125
A(37,36,40)	132.1185	A(32,37,36)	117.2315	A(32,37,61)	119.0431
A(36,37,61)	123.7253	A(35,38,39)	105.176	A(38,39,40)	113.6767
A(38,39,41)	122.8132	A(40,39,41)	123.5097	A(36,40,39)	106.7119
A(36,40,46)	124.5837	A(39,40,46)	128.6451	A(39,41,42)	125.5604
A(39,41,45)	123.685	A(42,41,45)	110.7545	A(41,42,43)	113.1554
A(41,42,62)	121.5211	A(43,42,62)	125.3234	A(42,43,44)	112.7957
A(42,43,63)	123.9038	A(44,43,63)	123.3004	A(43,44,45)	111.9142
A(43,44,64)	128.4471	A(45,44,64)	119.6387	A(41,45,44)	91.3801
A(41,45,48)	79.3565	A(44,45,48)	145.0939		

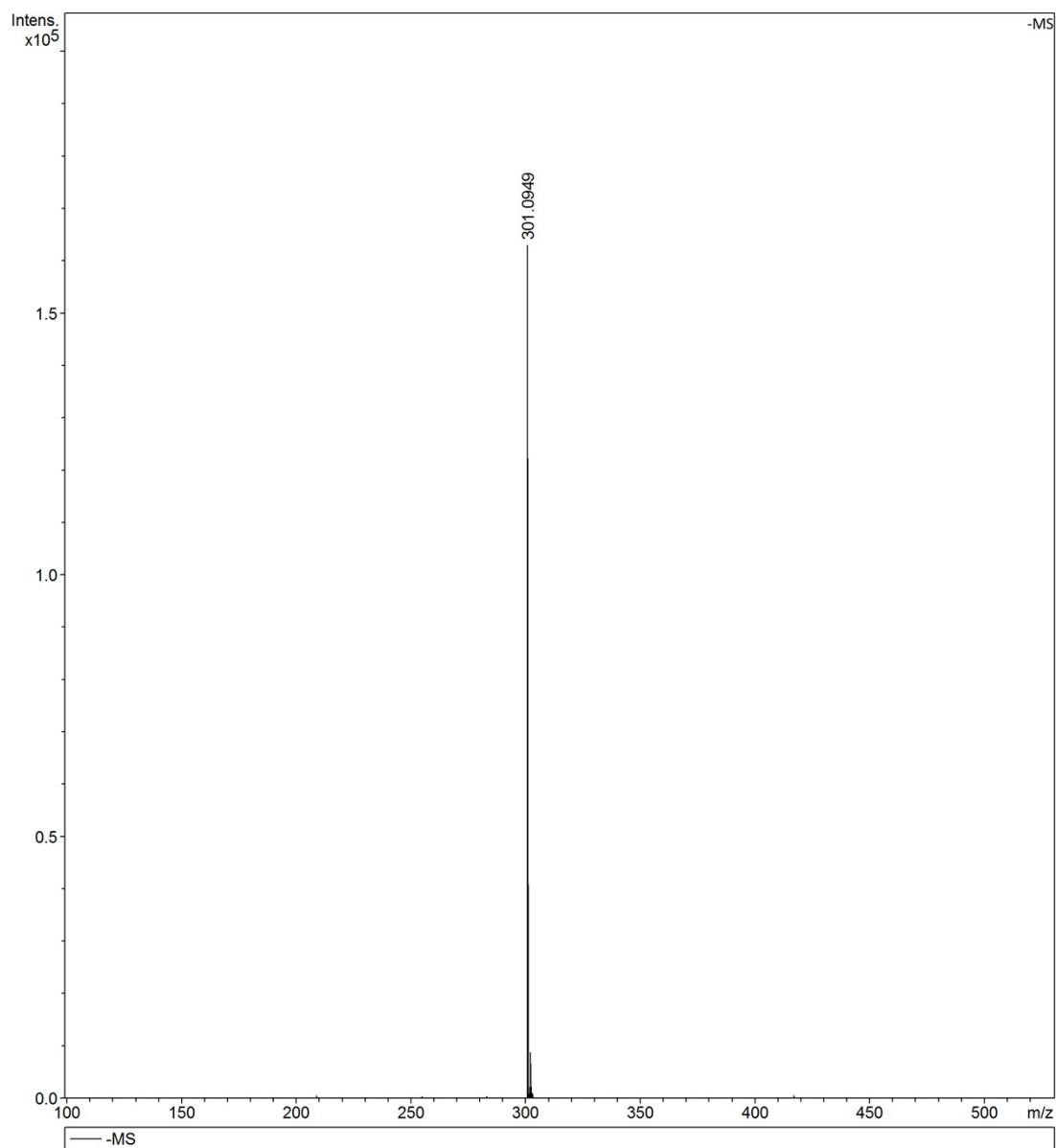


**Fig. S14** ESI-MS spectrum of **IM**.

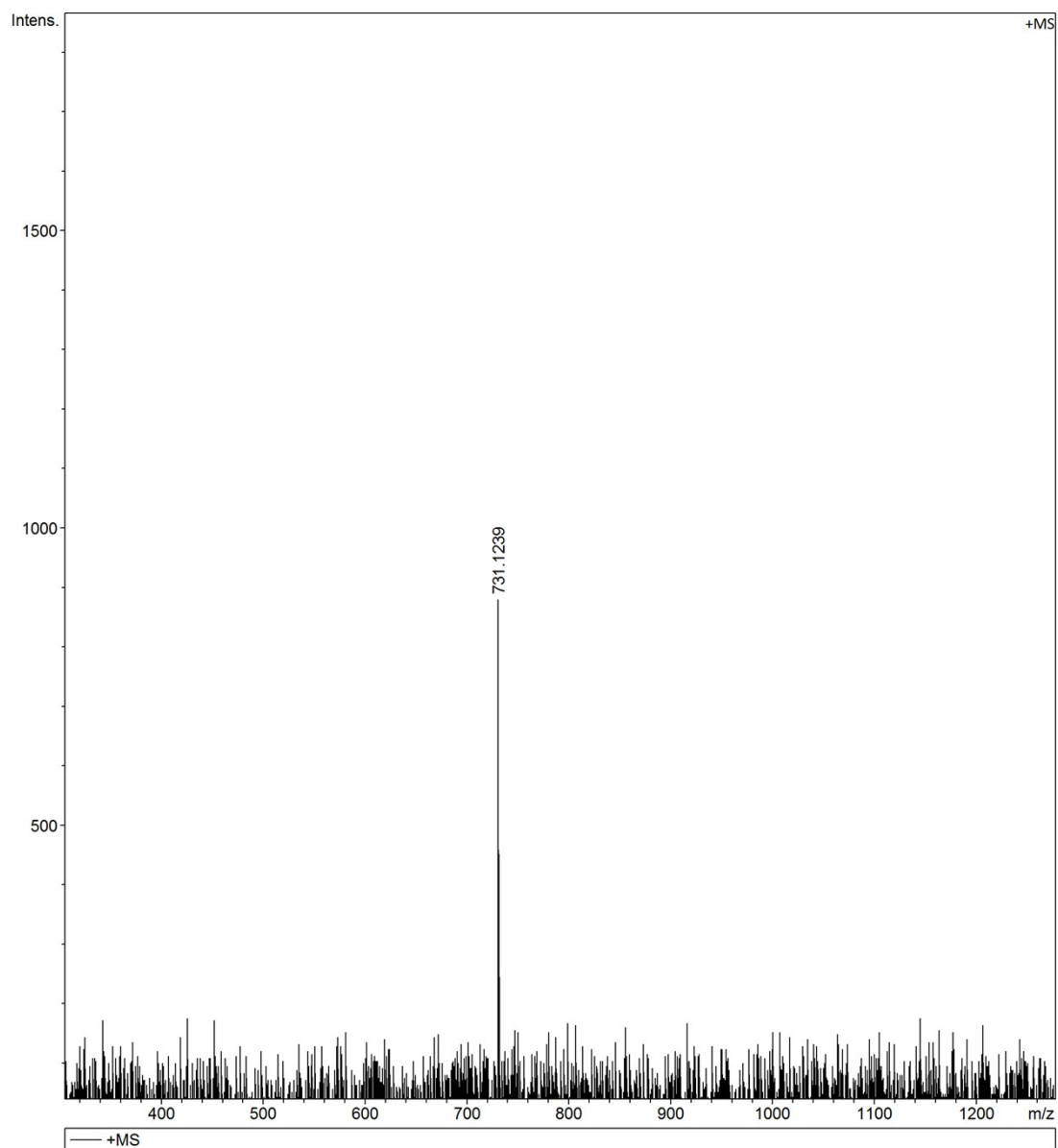


**Fig. S15** ESI-MS spectrum of **IM-Ag<sup>+</sup>**.

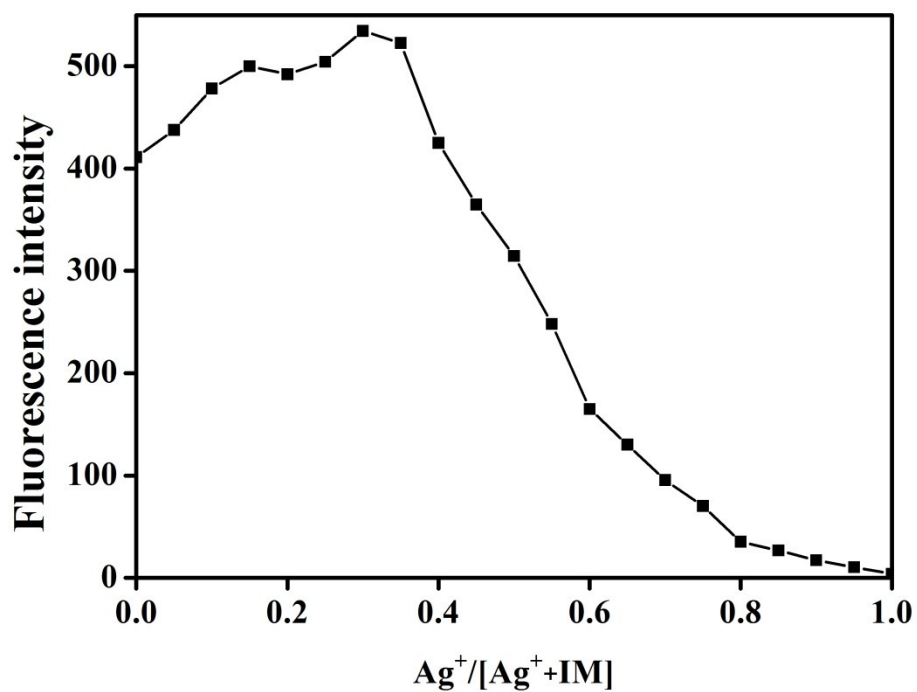


**Fig. S16** The Job's plot examined between  $\text{Ag}^+$  and **IM**, indicating the 2 : 1 stoichiometry, which was carried out by fluorescence spectra ( $\lambda_{\text{exc}} = 400 \text{ nm}$ ).

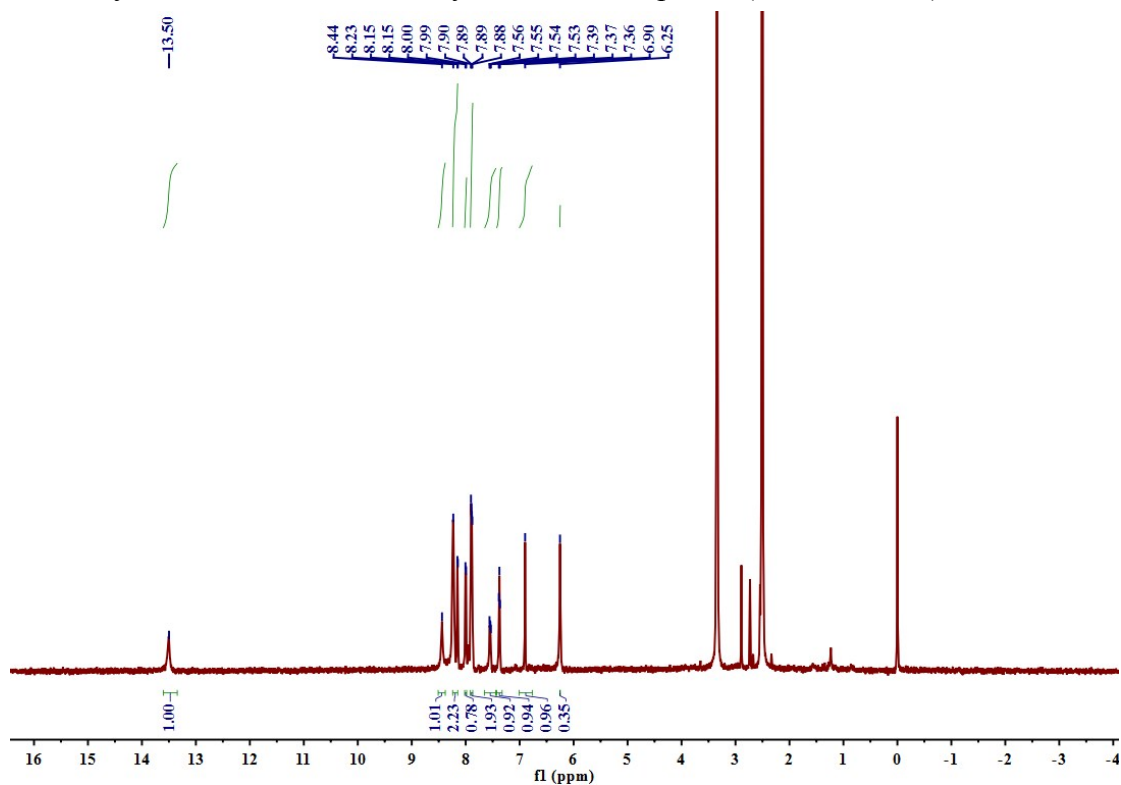


**Fig. S17**  $^1\text{H}$  NMR spectra of compound **IM**.

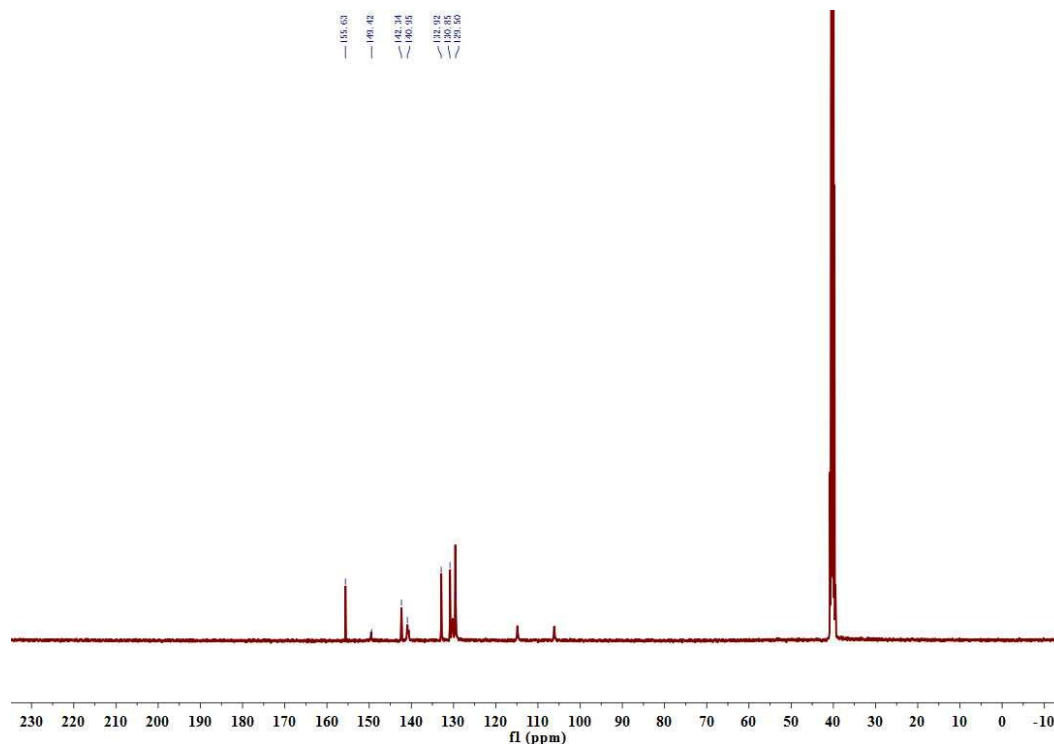


**Fig. S18**  $^{13}\text{C}$  NMR spectra of compound **IM**.

## References

- [1] C. Liu, S. Huang, H. Yao, S. He, Y. Lu, L. Zhao, X. Zeng, *RSC Adv.*, 2014, **4**, 16109–16114.
- [2] Y. -T. Wu, J. -L. Zhao, L. Mu, X. Zeng, G. Wei, C. Redshaw, Z. Jin, *Sens. and Actuators B: Chem.*, 2017, **252**, 1089-1097.
- [3] C. Chen, H. Liu, B. Zhang, Y. Wang, K. Cai, Y. Tan, C. Gao, H. Liu, C. Tan, Y. Jiang, *Tetrahedron*, 2016, **72**, 3980–3985.
- [4] Y. Jiang, W. Kong, Y. Shen, B. Wang, *Tetrahedron*, 2015, **71**, 5584–5588.
- [5] T. -B. Wei, H. L. Zhang, W. T. Li, W. J. Qu, J. X. Su, Q. Lin, Y. M. Zhang and H. Yao, *Chin. J. Chem.*, 2017, **35**, 1311-1316.